Potential of CF_3I Gas Mixture as an Insulation Medium in Gas-Insulated Equipment

L. Chen[1], P. Widger[1], M. S. Kamarudin[2], H. Griffiths[1], A. Haddad[1]
[1]Advanced High Voltage Engineering Research Centre, Cardiff University, UK
[2]Universiti Tun Hussein Onn, Johor, Malaysia
Chent3@cardiff.ac.uk

***Abstract*—SF_6 is a widely used gas medium in gas-insulated equipment. Due to the high global warming potential and long atmospheric lifetime of SF_6, there has been research into a new environmentally friendly replacement gas. This paper describes the research carried out at Cardiff University on CF_3I gas and its mixture as a substitute insulation medium for SF_6 in gas-insulated lines (GIL). A reduced-scale coaxial test system having the electric field properties of a full-scale 400 kV GIL system was fabricated. The design of the reduced-scale coaxial test system was simulated to ensure that the highest electric field would be along the center of the conductor. The coaxial prototype was then tested under a standard lightning impulse (1.2/50) in order to determine the 50% breakdown voltage for such a system when insulated with CF_3I gas mixture. It was found that CF_3I has the potential to replace SF_6 as an insulation medium in GIL. A full-scale short length GIL demonstrator is being assembled in the laboratory to evaluate further the feasibility of using a CF_3I gas mixture as an insulation medium.**

***Keywords*—Dielectric breakdown, gas insulated substations, gas insulation, impulse testing, SF_6.**

I. Introduction

In response to the Kyoto Protocol on climate change, governments worldwide have set ambitious targets to reduce greenhouse gas emissions. In high-voltage equipment, such as gas-insulated switchgear (GIS) and gas-insulated lines (GIL), SF_6 is the most commonly used dielectric gas medium. This is because SF_6 is chemically stable with a high arc interruption capability and a dielectric strength three times that of air at atmospheric pressure [1]. SF_6, however, is one of the six restricted greenhouse gases identified by the Kyoto Protocol due to the fact that its global warming potential (GWP), for a given time horizon of 100 years, is 23,900 times that of CO_2 [2]. Identifying alternatives to SF_6 for application in high-voltage gas-insulated equipment remains a tantalizing problem for researchers. There are gases that exhibit a higher dielectric strength than SF_6, but they all possess at least one negative characteristic, such as a high boiling point, high GWP, high toxicity, low dielectric strength, harmful by-products or voltage-withstand limitation.

An emerging candidate is Trifluoroiodomethane (CF_3I), a gas that is chemically inert and nonflammable and that has a dielectric strength that is 1.2 times higher than that of SF_6 [3]. The weak chemical bond C-I in CF_3I means that it decomposed quickly in the atmosphere, which is one of the reasons that CF_3I possesses a GWP of around 1, for a given time horizon of 100 years [4]. This gas was proposed initially by researchers as an alternative to SF_6 gas in high-voltage gas-insulated equipment. However, CF_3I does have limitations including a high boiling point, and the fact that it has to be used in low proportions as part of a binary mixture with CO_2 or N_2 to reduce the overall liquefaction temperature.

The aim of this research is to investigate the feasibility of implementing CF_3I gas mixture in GIL applications. To achieve this, a reduced-scale coaxial test system was designed, developed and fabricated. An initial experimental investigation was conducted for a 30/70% CF_3I/N_2 gas mixture to characterize the breakdown strength of this gas mixture in a quasi-uniform field represented by the coaxial geometry.

II. Experimental Setup and Test Method

A. Lightning Impulse Generator

Fig. 1 shows the test setup at Cardiff University using a 400 kV lightning impulse generator. A capacitive voltage divider with a ratio of 27,931 to 1 and 50 ns rise time was used to measure the lightning impulse voltage. A digital LeCroy wave-runner 64Xi was used to record the resulting waveform. To carry out the experiment, a pressure vessel made of mild steel was manufactured to withstand high gas pressure. The development process of the test rig is described in [5].

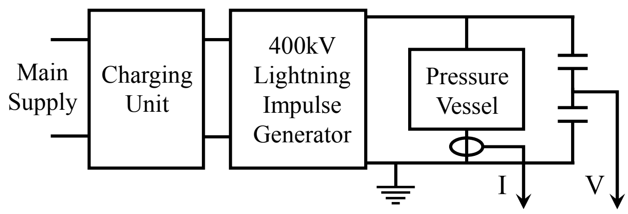

Fig. 1: Test circuit for standard 1.2/50 lightning impulse breakdown tests.

B. Up-down Method

The experimental work carried out in this investigation follows the IEC/BS EN 60060-1 standard [6]. For the breakdown tests, the up-down method was adopted. This is a testing method that determines the 50% breakdown voltage, U_{50}, of an electrode configuration within a small number of discharges; it requires minimal experimental time and achieves a good level of accuracy. For every test electrode arrangement, a minimum of 30 lightning impulses was applied during the experiments.

This work was supported through a PhD studentship from the Engineering and Physical Sciences Research Council (EPSRC) - Transformation of the Top and Tail of Energy Networks Grant [grant number EP/I031707/1].

III. Coaxial GIL Prototype Development

A. Design Principle

The geometric structure of the GIL is effectively a coaxial cylindrical electrode configuration, as can be seen in Fig. 2, where the outer conductor radius is R_a and the inner enclosure radius is R_b.

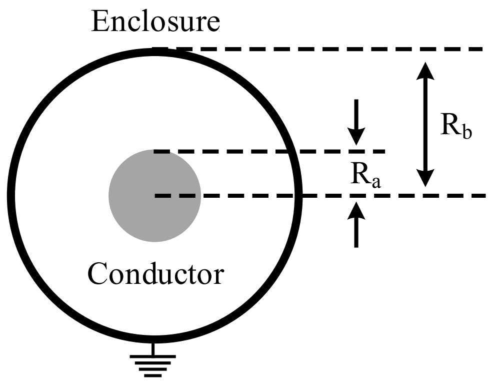

Fig. 2: Cross-section view of a coaxial geometry.

In a coaxial design, the highest electric field occurs along the surface of the inner conductor located at the center of the coaxial geometry, where breakdown is thus most likely to originate. Equation (1) is applied to determine the dimensions of R_a and R_b for the scaled prototype. The selections of R_a and R_b were based on the practical constraints of fitting the test system inside a pressure vessel and the voltage limitation of the high-voltage bushing of the vessel (approx. 170 kV lightning impulse).

$$E = \frac{U}{R_a \cdot \ln(R_b / R_a)} \tag{1}$$

When the voltage stress along the conductor reaches the breakdown field strength E_b, (1) can be re-written as (2).

$$U_b = E_b \cdot R_a \cdot \ln(\frac{R_b}{R_a}) \tag{2}$$

An important factor that needs to be taken into consideration for the design is the optimization of the quantity $\ln(R_b/R_a)$ [7]; a value of unity is considered the optimal ratio for gap distance and field uniformity in a coaxial geometry. Assuming E_b to be a constant value, then, by fixing R_b, the optimal design of a coaxial geometry can be achieved by $\ln(R_b/R_a) = 1$.

Existing high voltage GIL systems have adopted this optimal ratio for their geometric dimensioning, as can be verified from previous literature [8]. The report from AZZ CGIT, a major manufacturer of GIL worldwide, details the dimensions of all the GIL systems from a rated voltage of 145 kV to 1200 kV. The equivalent lightning impulse withstand voltages were plotted against the geometric ratios of the GIL, and these are shown in Fig. 3. It can be seen that the majority of the dimensions are between ratios of 1 to 2.718 (optimal) or 3. For the dimensions of 800 kV and 1200 kV rated GIL, however, the geometric ratio is much larger than for the GIL at a lower voltage rating. This indicates that at a very high voltage rating, it is possible that the factor of gap spacing takes precedence over the geometric field uniformity in the GIL.

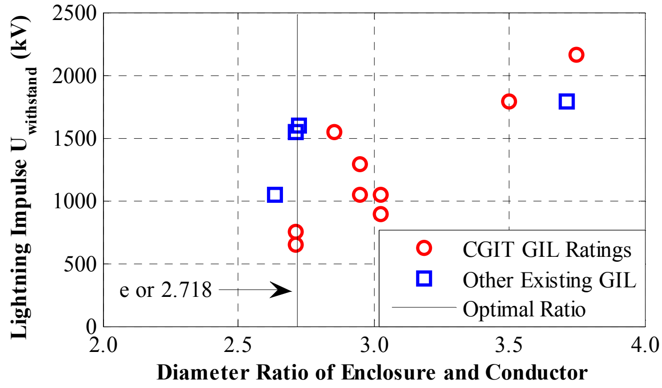

Fig. 3: Relationship between lightning impulse withstand voltage and dimensions in existing GIL systems.

B. Geometric Dimensioning of the Prototype

A coaxial geometry was designed using a 1 to 3 ratio for the conductor and the enclosure, which is a ratio similar to the majority of existing GIL systems at 400 kV.

Fig. 4 shows the proposed design geometry of the prototype. It can be seen that a curvature radius was added onto the inner wall. The curvature on the wall will ensure the gap distance widens towards the end of the enclosure, thereby reducing the likelihood of breakdown at the edges of the enclosure and avoiding regions of high electric field stress.

The conductor was designed to be positioned deeper into the support insulator. This way, the flashover distance between the conductor end and the enclosure wall was maximized.

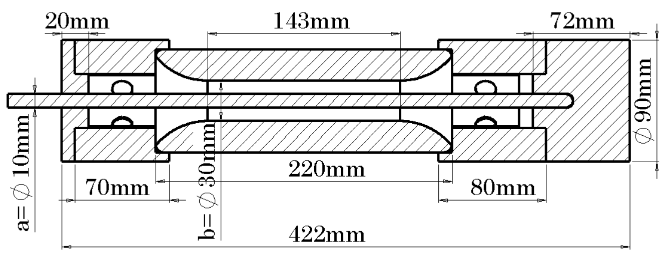

Fig. 4: Design of reduced-scale coaxial GIL test system. The values of "a" and "b" indicate the diameters corresponding to R_a and R_b.

IV. Simulation Modelling

The effective ionisation coefficients of different gases and gas mixtures were computed using BOLSIG+, which applies the two-term approximation of the Boltzmann equation [9]. Fig. 5 shows the pressure-reduced ionisation coefficient $(\alpha - \eta)$ as a function of E/p.

The critical reduced field strength, $(E/p)_{crit}$ of CF_3I and SF_6 at $(\alpha - \eta) = 0$ is consistent with experimental results reported in [3], which have shown that pure CF_3I has a dielectric strength around 1.2 times higher than that of SF_6. The steepness of the slope for SF_6 and CF_3I indicates that the two gases are relatively brittle, as a strong growth of ionisation would occur in the region where $E/p > (E/p)_{crit}$, especially in the presence of defects on the surface of gas-insulated equipment [1]. The result for the 30/70% CF_3I/N_2 gas mixture was found to be in good agreement with the published result in the literature [10]. The $(E/p)_{crit}$ of the 30/70% CF_3I/N_2 gas mixture is 6.27 kV/mm/bar, which is comparably higher than the $(E/p)_{crit}$ of the 30/70% CF_3I/CO_2 gas mixture of 5.53 kV/mm/bar. For this reason, the 30/70% CF_3I/N_2 gas mixture was used for the experimental work carried out in this paper.

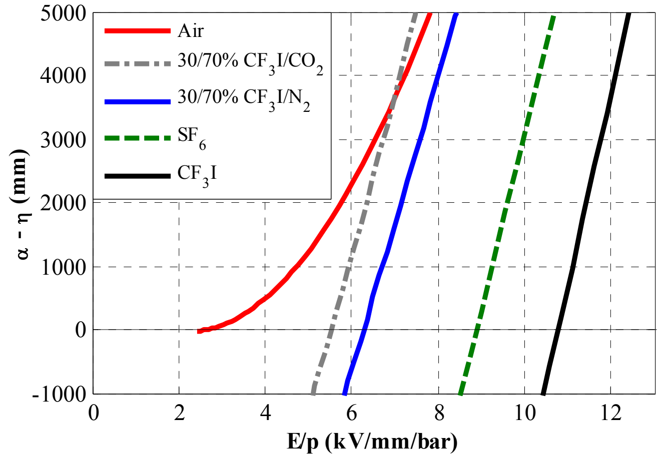

Fig. 5: Effective ionisation coefficients in pure gases (Air, SF_6 and CF_3I,) and gas mixtures (30/70% CF_3I/N_2 and 30/70% CF_3I/CO_2).

In a coaxial test system with a geometric ratio $R = R_b/R_a$, when the field strength on the conductor R_a exceeds the critical field strength of the gas mixture, the corona inception can occur at a voltage $U > U_{inception}$. Assuming that no leader channel was formed, the streamer breakdown voltage U_S can be calculated using (3).

$$U_S = E_{crit} \cdot (R_b - R_a) \tag{3}$$

A simulation of the coaxial model was carried out using COMSOL to identify regions of high electric field. As can be seen in Fig. 6, the maximum electric field can be seen to occur along the center region of the conductor. The field strength decreases towards both ends of the enclosure as the gap distance widens.

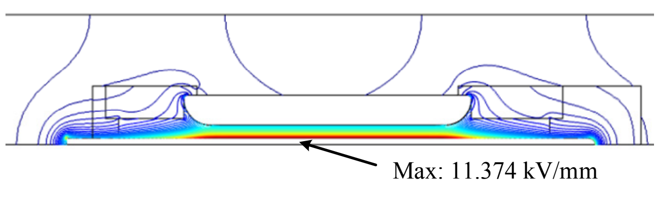

Fig. 6: Plot of electric field distribution showing the maximum electric field at the center of the conductor.

The fabricated prototype is shown in Fig. 7. Both the enclosure and the conductor are made out of aluminium, and they are kept apart by insulators made out of polypropylene. As can be seen on the photo, there are several holes in the insulators; these are introduced to allow the CF_3I gas mixture to circulate freely into the coaxial test system. A 10 mm thread was made on the tip of the conductor for connecting it to the bushing.

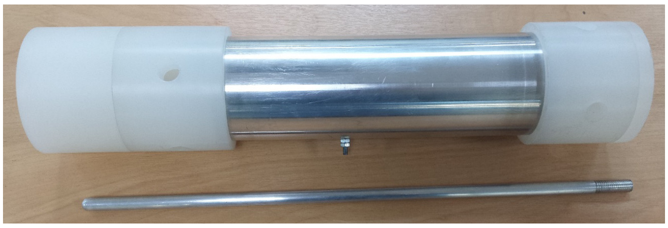

Fig. 7: Photograph of the reduced-scale coaxial test system.

V. Results and Discussions

Keeping the enclosure diameter constant, two different-sized inner conductors were fabricated to investigate the effect of gap spacing in coaxial electrode arrangements. It is stated in the literature [5] that the highest breakdown voltages can be reached with ratios of R_b/R_a, which are very close to the optimum value. It can be seen in Fig. 8 that there is a linear relationship between the breakdown voltage and gas pressure, irrespective of the gap spacing. As pressure increases, the voltage will increase less linearly, as has been observed by other researchers [11]. A coaxial geometry of R_a/R_b having a 15/30 mm has a higher geometric field uniformity than a 10/30 mm coaxial geometry. However, it will also lead to a lower breakdown voltage due to the gap spacing between the inner and outer coaxial cylinders being smaller.

The pressure-reduced maximum breakdown field strength $(E_{max}/p)_B$ is given by the field strength at the inner cylinder when $U_b = U_{50}$. If we assume that this breakdown field strength is exceeded at the inner cylinder at breakdown, then (4) can be utilised in order to calculate the $(E_{max}/p)_B$ values of the 30/70% CF_3I/N_2 gas mixture.

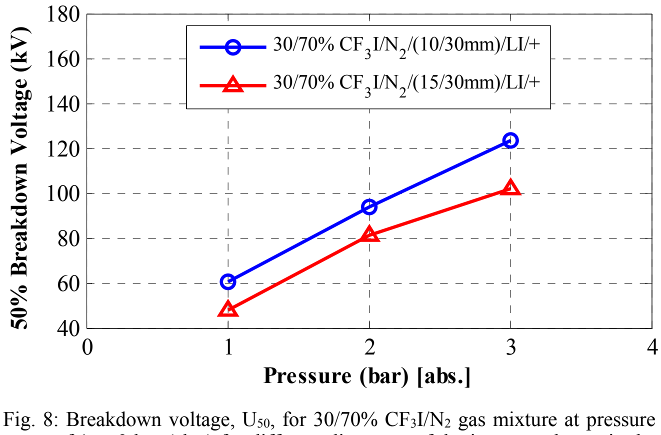

Fig. 8: Breakdown voltage, U_{50}, for 30/70% CF_3I/N_2 gas mixture at pressure range of 1 to 3 bar (abs.) for different diameters of the inner conductor in the coaxial test configuration for positive lightning impulse.

$$(E_{max}/p)_B = \frac{U_{50}}{R_a \cdot \ln(R_b/R_a) \cdot p} \tag{4}$$

The experimental $(E_{max}/p)_B$ values were converted using (4), and these are plotted in Fig. 9 for the 30/70% CF_3I/N_2 gas mixture. The $(E_{max}/p)_B$ values of the 30/70% CF_3I/N_2 gas mixture for 10 mm and 15 mm conductor diameters show the

$(E_{max}/p)_B$ slope gradually decreasing to $(E/p)_{crit}$ of the gas mixture (6.27 kV/mm/bar), as can be seen in Fig. 5. Further experimental work is required on a bigger coaxial geometry and on conductor/enclosure ratios that provide lower geometric field uniformity.

Two of the coaxial geometries that were investigated in this work had similar geometric ratios to the 32/96 mm and 50/96 mm geometries reported in [11] for SF_6 gas. A comparative study was carried out, and the results are shown in Fig. 9. A similar trend can be seen from the results of both sets of coaxial test systems. The set of systems with a 1/3 ratio (close to optimal) has comparably higher $(E_{max}/p)_B$ values and requires higher pressure to give values lower than the $(E/p)_{crit}$ value. It is important to design the GIL system to be well below the $(E/p)_{crit}$ of the chosen gas mixture to avoid a complete breakdown of the insulation.

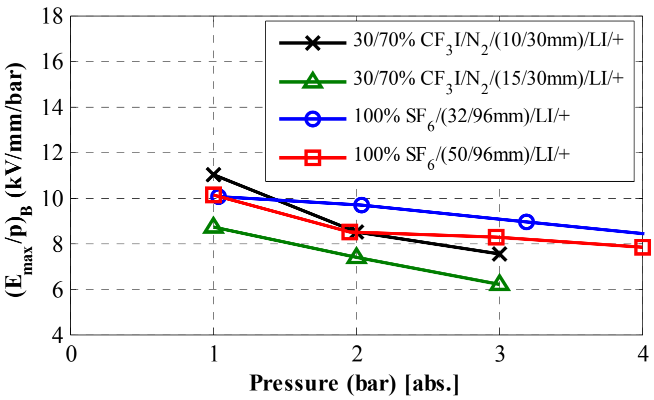

Fig. 9: Pressure-reduced maximum breakdown field strength, $(E_{max}/p)_B$, as a function of pressure for SF_6 and 30/70% CF_3I/N_2 for coaxial test systems with geometric ratios of 1/2 and 1/3 and for positive lightning impulse.

Table I shows a comparison of electric field values. Assuming that, at atmospheric pressure, the primary streamer bridges the inter-electrode gap in the coaxial test system, a streamer breakdown may be initiated when $U_b = U_S$. This value is then applied in (1) to calculate the E_{max}. The calculated U_S was also used in COMSOL to obtain the electric field distribution and the simulated E_{max} value. Finally, the measured U_{50} was converted using (4) into $(E_{max}/p)_B$ value. It can be seen from Table I that all three E_{max} values are in good agreement.

However, for higher gap distances and pressures, there will be a potential drop in the measured U_{50}. This may be due to the formation of a self-propagating leader channel, which then initiates a leader breakdown across the inter-electrode gap. A mathematical model is currently being developed to explain the drop in potential and its correlation to the streamer/leader phenomenon.

TABLE I. COMPARISON OF CALCULATED, SIMULATED AND MEASURED MAXIMUM ELECTRIC FIELD VALUES.

Calculated E_{max}	11.41 kV/mm/bar
Simulated E_{max}	11.37 kV/mm/bar
Experimental $(E_{max}/p)_B$	11.02 kV/mm/bar

VI. CONCLUSION

The breakdown characteristics of the 30/70% CF_3I/N_2 gas mixture were experimentally investigated in a reduced-scale coaxial test system using conductors with a diameter of 10 mm and 15 mm and a fixed inner enclosure diameter of 30 mm.

The results have demonstrated the potential of using a CF_3I gas mixture to replace SF_6 gas as an insulation medium. Further experimental investigations are required on various CF_3I gas mixtures and coaxial geometries. It is hoped that future work will determine an appropriate CF_3I gas mixture candidate to be used in GIL applications.

The next step of this research is to construct a full-scale 400 kV GIL demonstrator. Extensive testing of this system will provide a better indication of whether CF_3I gas and its mixtures can be used in full practical GIL systems.

ACKNOWLEDGMENT

The authors would like to thank Professors K. Hidaka and A. Kumada of Tokyo University, Japan, for the fruitful discussions.

REFERENCES

[1] A. Haddad and D. Warne, "SF_6 insulation systems and their monitoring", *Advances in High Voltage Engineering,* London, UK: IET, ch.2, pp.38–45, 2009.

[2] "Inventory of U.S. Greenhouse Gas Emissions and Sinks: 1990-2000", *Office of Atmospheric Programs, U.S. Environmental Protection Agency,* Washington (USA), 2002.

[3] J. Urquijo, A. Mitrani, G. Ruiz-Vargas and E. Basurto, "Limiting field strength and electron swarm coefficients of the CF_3I-SF_6 gas mixture", *Journal of Physics D: Applied Physics*, vol.44, no.34, pp.342001, 2011.

[4] L. G. Christophorou and J. K. Olthoff, "Electron Interactions with CF_3I", *Journal of Physical and Chemical Reference Data*, vol.29, no.4, pp.553–569, 2000.

[5] L. Chen, P. Widger, C. Tateyama, A. Kumada, H. Griffiths, K. Hidaka and A. Haddad, "Breakdown characteristics of CF_3I/CO_2 gas mixtures under fast impulse in rod-plane and GIS geometries", *19th International Symposium on High Voltage Engineering*, 547, Pilsen (Czech Republic), 2015.

[6] "IEC/BS EN 60060-1: High-voltage test techniques – Part 1: General definitions and test requirements", *British Standard Institutions*, 2010.

[7] E. Kuffel, W. S. Zaengl, and J. Kuffel, *High Voltage Engineering - Fundamentals*, 2nd ed., Oxford, UK: Newnes, 2000.

[8] "Compressed Gas Insulated Transmission Bus Systems – Proven Solutions for Power Transmission", *AZZ CGIT Technical Brouchure 001*, Westborough (USA), 2004.

[9] G. J. M. Hagelaar and L. C. Pitchford, "Solving the Boltzmann equation to obtain electron transport coefficients and rate coefficients for fluid models", *Plasma Sources Science and Technology*, vol.14, no.4, pp.722–733, 2005.

[10] D. Tanaka, A. Kumada, and K. Hidaka, "Numerical Simulation of Streamer Development in CF_3I-N_2 Gas Mixtures", in *17th International Symposium on High Voltage Engineering*, A–14, Hannover (Germany), 2011.

[11] S. Menju, H. Aoyagi, K. Takahashi, and H. Qhno, "Dielectric Breakdown of High Pressure SF_6 in Sphere and Coaxial Cylinder Gaps", *IEEE Transactions on Power Apparatus and Systems*, vol.PAS–93, no.5, pp.1706–1712, 1974.